CONDENSATE DISPLACEMENT MECHANISMS IN LOW PERMEABILITY ROCKS

Mahmood Al Harrasi[a], Carlos Grattoni[b], Quentin Fisher[a] and Suleiman Al-Hinai[c]

[a] *School of Earth and Environment, University of Leeds, Leeds, LS2 9JT*

[b] *Rock Deformation Research, University of Leeds, Leeds, LS2 9JT, UK*

[c] *Petroleum Development of Oman, MAF, Sultanate of Oman, P.O. Box 81, PC: 100*

This paper was prepared for presentation at the International Symposium of the Society of Core Analysts held in Noordwijk, The Netherlands 27-30 September, 2009

ABSTRACT

Gas condensate reservoirs are becoming increasingly important due to the growing world dependence on gas supply and the high value of condensate in the market place. The current understanding of fluid flow behaviour within tight rocks is limited due to the limited data available. Furthermore, the lack of accurate relative permeability data for tight rocks in both gas and gas condensate reservoirs represents a significant knowledge gap.

The production from a gas-condensate reservoir leads to an isothermal pressure fall causing liquid drop-out called 'retrograde condensate' that first appears around the well-bore. A significant condensate build-up occurs near the well-bore which causes a reduction in gas relative permeability, a phenomenon called 'condensate blockage'. The significance of condensate blockage in low permeable rocks is still unclear. This study aims to provide the essential understanding of the flow mechanisms of condensate blockage in porous media. A pore-scale experimental study has been performed to give an insight to the condensate blockage. Glass micromodels with different pore structure (e.g. different pore aspect ratio, pore size, coordination number etc.) have been used to test the impact of porous media properties. A fluid system of three components, which allow systematic variation of the interfacial tension (IFT), has been used to investigate gas condensate fluid configurations and dynamic behaviour. The results showed that condensate blockage depends on pore size and coordination number. The porous media characteristics play a significant role on the degree of blockage that condensate imposes to the gas flow through pore spaces. A discussion of the use of the existing correlations for predicting relative permeability will be examined and checked against the experimental observations.

INTRODUCTION

This paper addresses the physics of multiphase flow in porous media for systems of low interfacial tension where the characteristics of multiphase flow for gas-condensate systems will be emphasized. A gas-condensate reservoir is initially a single-phase (gas) until pressure falls below the dewpoint. Then a second phase (called condensate) is created which leaves smaller path flow for the gas and thus decreasing its production. Understanding the behaviour of condensate systems requires pore-scale perspective of

the flow dynamics and distribution of both phases, i.e. gas and condensate. This behaviour is affected by some parameters including interfacial tension, wettability, pore geometry and phase saturation. For a gas condensate system, the gas relative permeability at high IFT can be divided into two distinct regimes: firstly of low condensate saturation and secondly of high condensate saturation. The condensate in the first regime flows on the wall surface and forms bridges that close and open in the second regime. As a result, a sharp drop in gas relative permeability occurs in the second regime.

This paper focuses on the effects of pore geometry on the flow behaviour which will give an insight to the effect that permeability has on condensate blockage phenomena. Little work has been found in literature for the effect of pore geometry on gas-condensate systems. Micromodels have proved their capability to study multiphase flow behaviour in porous media. Previous researchers have studied the behaviour of gas-condensate systems in micromodels by creating the condensate in-situ by either using partially miscible binary systems [1] or gas mixtures [2]. However, this study will introduce, for the first time, condensate by injection. Therefore, the saturation of each phase can be varied by changing the fractional flow.

MATERIALS AND EXPERIMENTAL TECHNIQUES

Fluid System

A three component fluid system with an upper critical solution temperature (UCST) has been used in this study (**Figure 1**). This ternary fluid consists of cyclohexene, isopropyl alcohol, and water (CIPAW). The three components are mixed to give two-phase mixtures of different interfacial tensions, varying from high IFT, 24.2 mN/m (at 0 % v/v IPA concentration) to ultra-low IFT, 0.03 mN/m (at 50% v/v IPA concentration) [3]. The upper phase ‘light phase, LP’ is cyclohexene-rich and the lower phase ‘heavy phase, HP’ is water-rich (**Figure 1**). According to the density and viscosity contrasts between the two phases, the light phase represents ‘gas’ and the heavy phase represents ‘condensate’. Blue dye (darker colour in this paper) was used for the lighter phase ‘gas’ for clear distinction between the two phases. Therefore, this modelling technique can be used to test two-phase flow behaviour at different interfacial tensions. Physical properties are given in **Table 1** and give the advantage of possible flow quantification.

Micromodels

Micromodels are transparent etched glass networks that represent the structure of idealized porous media consisting of pores interconnected by throats. These micromodels have proven track record to study some pore-scale events such as fluid distributions [4], capillary and surface phenomena [5] and the critical behaviour of partially miscible binary fluids [1,5,6]. Kamal [7] described the design and construction of micromodels and some of their applications have been reported by Dawe and Grattoni [8]. Although micromodels do not represent real rocks because of the two-dimensional (2-D) nature, they have demonstrated strengths in capturing some pore-scale events that would occur in three-dimensional (3-D) porous media. This study has used micromodels of different pore sizes and wettability conditions (**Figure 2**).

Apparatus and Procedure

Different fluid mixtures and micromodels were used in this experimental work. The micromodel is put under a microscope which is fitted to a colour high speed video camera (Adimec 1000C DUAL). A lamp is used to illuminate the pore-scale events taken place. The two phases are injected using two syringe pumps (World Precision Instruments, model number: ALADDIN-1000). The camera records video clips that are transferred directly to a data acquisition system on a computer (National Instruments Measurement & Automation Explorer and LABVIEW8). Snapshots are taken from the video clips using video programs programs (Able Video Snapshot 1.5.6.15 from Graphic Region). **Figure 3** shows a schematic of the micromodel experimental set-up.

The micromodel is initially fully saturated with light phase, LP (gas) and then heavy phase, HP(condensate) is injected at increasing fractional flow until injecting 100% of HP. The total flow rate used in the experiments is 0.1 ml/min. This represents the mechanism that occurs in gas condensate reservoirs where the reservoir is initially saturated with a single phase into which a second phase starts to flow. At each fractional flow, enough pore volumes were injected to reach steady state conditions.

IMPACT OF INTERFACIAL TENSION

Two-phase flow experiments were carried out to test the effect of interfacial tension on gas-condensate dynamic behaviour. The micromodels used are oil-wet where the surface is coated by the HP (condensate) and the LP (gas) occupies the outer of the pores. The results showed that for high IFT (24.2 mN/m), LP has no ability to deform when passing through constrictions and thus is trapped in the pores. For ultralow IFT (0.03 mN/m), both phases flow almost as a single phase and as a result the flow is unrestricted.

The light phase shows different flow mechanisms when the interfacial tension is intermediate (1.5 mN/m). These mechanisms facilitate the flow of gas and therefore increase its relative permeability. These mechanisms are dripping, upstream subdivision and pinch-off, elongation and snap-off. **Figure 4** shows the dripping mechanism where a ganglion splits into smaller droplets at the entrance of a throat (constriction). This process continues until the large ganglion decreases its size to a droplet that can pass through the throat. When a large ganglion comes to a junction of a pore, it stretches into the two throats of the pore. The ganglion is pinched off by another upstream ganglion at the pore junction. This helps splitting of the large ganglion and thus improves its flowing potential (**Figure 5**). Another mechanism is elongation where the light phase deforms through more than single pore. The elongated ganglion gets thinned until snap-off occurs (**Figure 6**). The flow of the LP is emulsion-like for the intermediate IFT. For low IFT (0.6 mN/m and 0.1 mN/m), the flow is more ganglion-like where deformation occurs with less snap-off (more continuity) (**Figure 7**).

The saturation of the phases can be changed by varying the fractional flow of each phase. Heavy phase can flow on the surface or as long thin filament stretching along several pores when its saturation is low (i.e. its fractional flow is 2%) at intermediate to low interfacial tensions (**Figure 8**). The thin strand remains attached to the upstream original upstream grain and consequently its velocity is less than that of the light phase.

The residual gas saturation increases as the interfacial tension increases due to stronger capillary holding forces (**Figure 9**).

The above mechanisms have been observed by other researchers where condensate is created in-situ by pressure depletion using temperature-induced separation using a partial miscible binary system [1] or hydrocarbon gas mixture [2]. This indicates that the mode of the experiment (simultaneous injection as this work versus in-situ condensation as other works) has no influence on phases distribution and dynamic behaviour.

Image analysis tools are used to calculate the saturation of the phases at each fractional flow. The relative permeability ratio can be calculated from the following equation

$$\frac{kr_g}{kr_o} = \frac{Q_g\,\mu_g}{Q_o\mu_o}$$

A plot of (kr_g/kr_o) ratio versus heavy phase saturation (S_o) shows that as the interfacial tension decreases the ratio increases, at a certain S_o. However, there is a crossover of the trend at certain condensate saturation (S_o) (**Figure 10**). This crossover indicates a change in the dynamic behaviour of the phases at that saturation (S_o). The same trend was observed by Al-Wahaibi et al. [9] using the same fluid system in glass beadpacks.

Capillary number is the ratio of viscous to capillary forces on a pore scale. It is common to include capillary number in gas-condensate relative permeability functions. The viscous force can be defined by either pressure drop or as viscosity-velocity product. Using viscosity-velocity definition, the cross-sectional area can be approximated as a product of micromodel width and pores depth. In our experiments, for the first time, both phases are injected at constant fractional flow and thus will result in different capillary numbers for the two phases. Therefore, capillary number can be defined as a product of cross-sectional area:

$$N_c.A = \frac{\mu_\alpha\, Q_\alpha}{\sigma}$$

Where

N_c: capillary number, dimensionless

A: cross-sectional area, m^2

μ_α: phase viscosity, Ns/m^2

Q_α: phase flow rate, m^3/s

σ: interfacial tension, N/m

Thus, for mixtures of IFT between 1.5 mN/m and 0.1 mN/m using micromodel 1, capillary number with 0.1 ml/min flow rate for each phase is of order 10^{-4} to 10^{-2}. This capillary number range represents the conditions near wellbore region [10]. Therefore, according to the results found in this work, a change in flow behaviour occurs at critical capillary number of 10^{-4} which is typical for a non-wetting phase in sandstones [11].

PORE GEOMETRY EFFECT

When micromodels of smaller pore spaces (MM2) and (MM3) are used, the mechanisms of pore hopping and filament flow of the heavy phase are more pronounced. The flow mechanisms of the light phase (gas) as shown above for larger pores are less efficient for smaller pores. For high IFT, the heavy layers on the grains bridged across the throats and thus blocking the way of the light phase (gas). However, as IFT gets lower, the attached heavy layers are not strong enough to block the flow of the light phase which can still flow as long strand through the throat (**Figure 11**). This may explain the shift of the behaviour crossover point towards higher (S_o) for smaller pores (or lower permeability). This will be shown later in this section. From the plots of (kr_g/kr_o) ratio versus condensate saturation (**Figures 12 and 13**), it has been noticed that less condensate saturations are needed to cause the same (kr_g/kr_o) ratio for smaller pores. This is clearly observed for low IFT where the flow of light phase (gas) through a throat is still possible even at high heavy phase saturation. Similar experiments have been performed on micromodels with different geometry and coordination number. However, they will not be shown here for paper size reasons.

The effect of miscibility on relative permeability can be described by different models. The Coats model [12] uses the interfacial tension as the controlling parameter and is still used in many commercial simulators. Coats correlation is an interpolation between miscible and immiscible relative permeability curves with the interfacial tension used as the weighting function. Further details on the model can be found in [12].

The model was fitted to some base curves, obtained from the literature, representing results from samples of different permeabilities: 1314 mD [13], 83 mD [14], 20 mD [13] and 0.136 mD. The relationship between the crossover point and permeability (**Figure 14**) shows that as permeability decreases the (S_o) crosspoint increases. However, the (kr_g/kr_o) crosspoint decreases as the permeability decreases.

IMPACT OF WETTABILITY

Figure 15 shows that the glass grains are wetted by the light phase (gas) whereas the heavy phase flows in the bulk of the pore spaces. Initially the heavy fluid is separated and isolated as ganglion or droplets. As the saturation of the heavy phase increases, it becomes more connected and hence a continuous flow path is established. The heavy phase flows as discrete droplets, i.e. emulsions, when the interfacial tension is low (0.1 mN/m). The size of the droplets of the heavy phase at low interfacial tension is very small and their size is smaller than that of pore throat size. At higher IFT, the flow of the heavy phase is ganglion-emulsion-like with hard deformation.

CONCLUSIONS

1. Micromodel experiments with liquid-liquid fluids are a useful tool to visualize pore-scale events for gas condensate systems in order to measure quantitative and qualitative results.

2. The two regimes in the gas relative permeability have been observed and are attributed to two distinct flow behaviours: filament flow of condensate on the grains or as long thin strands across several pore bodies and bulk flow of condensate where condensate breaks-up the flow of gas phase through the formation of bridges.

3. A change in behaviour occurs at larger condensate saturation for micromodels of smaller pore sizes.

4. A change in gas condensate behaviour occurs above a critical capillary number of 10^{-4}.

5. The mechanisms observed in laboratory tests by simultaneous flow of gas and condensate are similar to those observed by other researchers where condensate is created in-situ.

6. Wettability of porous media has a significant effect on fluids configuration.

ACKNOWLEGEMENTS

The first author would like to thank Petroleum Development Oman (PDO) for funding this PhD research. The authors wish to thank Dr Nik Kapur from Mechanical Engineering Department, Leeds University, for providing the laboratory facilities.

REFERENCES

1. Gray, J. and Dawe, R.," Modeling Low Interfacial Tension Hydrocarbon Phenomena in Porous Media", SPE 19696-PA (1991).
2. Danesh, A., Henderson, G. and Peden, J., "Experimental Investigation of Critical Condensate Saturation and Its Dependence on Interstitial Water Saturation in Water-Wet Rocks", SPE 19695-PA (1991).
3. Al-Wahaibi, Y., Grattoni, C., Muggeridge, A., "Physical properties (density, viscosity, surface tension, interfacial tension, and contact angle) of the system isopropyl alcohol plus cyclohexene plus water", J CHEM ENG DATA, (2007) **52**, 548 - 552.
4. Dullien, F., Lai, F., and MacDonald, I., "Hydraulic continuity of residual wetting phase in porous media", J. Colloid Interface Sci.,(1986) **109(1)**, 201-218
5. Williams, J. and Dawe, R., "Critical Behavior of Phase Separating Mixtures in Porous Media" Journal of Colloid and Interface Science, (1987)**117(1)**.
6. Dawe, R. and Grattoni, C., "Fluid flow behaviour of gas-condensate and near-miscible fluids at the pore scale" Journal of Petroleum Science and Engineering, (2007) **55(3-4)**, 228-236.
7. Ahmed K., "Some Effects of Wettability and Fluid Properties on Immiscible Displacement in Porous Media" PhD Thesis, Imperial College, London (1990).
8. Dawe, R. and Grattoni, C., "The Visualisation of The Pore Scale Physics of Hydrocarbon Recovery from Reservoirs" First break, (1998) **16(11),** 371-386.
9. Al-Wahaibi, Y., Muggeridge, A. and Grattoni, C., "Experimental and Numerical Studies of Gas/Oil Multicontact Miscible Displacements in Homogeneous Porous Media", SPE 92887-MS (2005).

10. Mott, R., Cable, A. and Spearing, M., "A New Method of Measuring Relative Permeabilities for Calculating Gas-Condensate Well Deliverability", SPE 56484-MS (1999).
11. Pope, G., Wu, W., Narayanaswamy, G., Delshad, M., Sharma, M. and Wang, P., "Modeling Relative Permeability Effects in Gas-Condensate Reservoirs With a New Trapping Model" SPE 62497-PA (2000).
12. Coats, K., "An equation of state compositional model", *SPE J.* (1980) **20 (5)**, 363–376.
13. Morgan, J. and Gordon, D.,"Influence of Pore Geometry on Water-Oil Relative Permeability", SPE 2588 (1970).
14. Bardon, C. and Longeron, D.,"Influence of Very Low Interfacial Tension on Relative Permeability",SPE 7609-PA (1980).
15. Washburn, E., Graham, C., George, B. and Laurence, F., "The Ternary Systems Involving Cyclohexene, Water, and Methyl, Ethyl and Isopropyl Alcohols", Journal of the American Chemical Society, (1940) **62(6)**, 1454:1457.

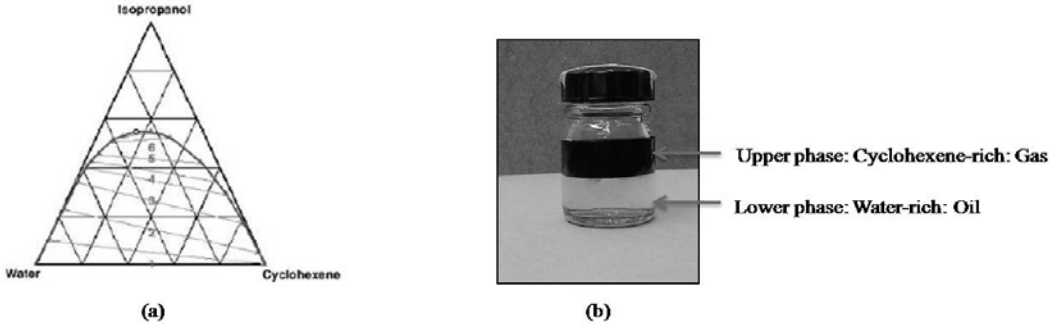

Figure 1. (a) Ternary phase diagram at 20 ^{o}C of isopropanol-water-cyclohexene (after [15]) (b) Picture of fluid mixture 3 (1.5 mN/m) shows the light phase (gas) in blue (dark colour) and the heavy phase (condensate) colourless.

Table 1. Interfacial tension of the fluid mixtures prepared with the physical properties of the two phases: cyclohexene layer and water layer (after [3]).

MIXTURE	COMPONENTS % (v/v)			IFT, mN/m	Density, gm/cc		Viscosity, cp	
	IPA	Water	Cyclohexene		Cyclohexene layer	Water layer	Cyclohexene layer	Water layer
1	0	50	50	24.2	0.8102	0.9982	0.668	1.033
2	16	42	42	6.9	0.8085	0.9691	0.669	2.582
3	28	36	36	1.5	0.8083	0.9441	0.763	3.304
4	36	32	32	0.6	0.8082	0.9286	0.978	3.601
5	44	28	28	0.1	0.808	0.9085	1.5447	3.619
6	50	25	25	0.03	0.82	0.8956	1.844	3.7

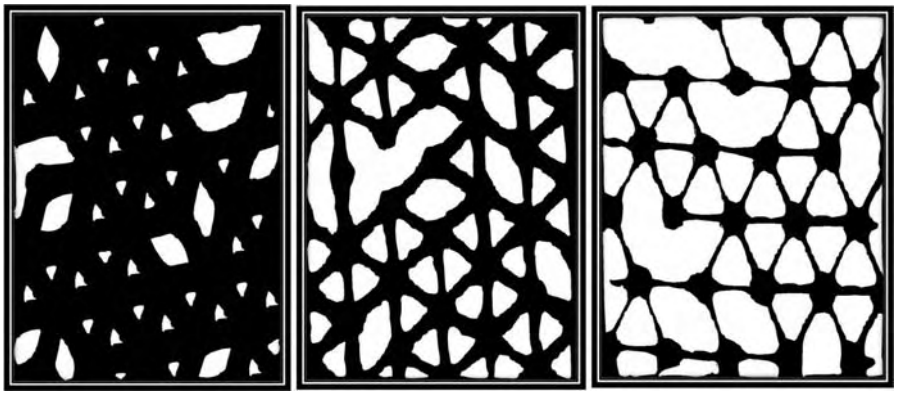

(MM1) (MM2) (MM3)

Figure 2. Micromodels of different pore sizes have been used. (MM1) large pore size (MM2) intermediate pore size and (MM3) small pore size.

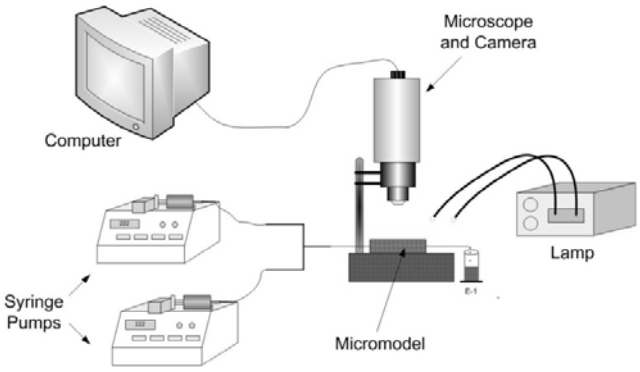

Figure 3. Schematic diagram of the micromodel experiment set-up. The fluid system is injected through the micromodel by syringe pumps. The microscope records the visual events which can be seen via a data acquisition system on a computer.

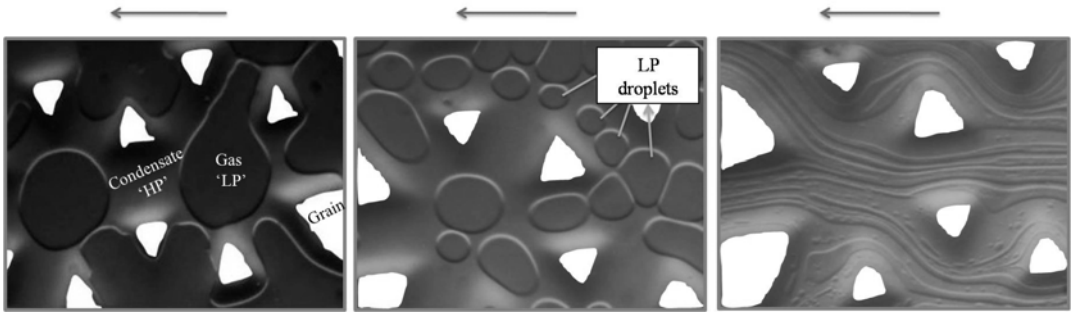

Figure 4. Left picture shows trapping at 24.2 mN/m IFT. Middle picture shows dripping mechanism of LP where a large ganglion is splitting into smaller droplets for 1.5 mN/m IFT. Right picture shows almost unrestricted flow for 0.03 mN/m. All pictures are on MM1 micromodel and the fractional flow of condensate ($F_{condensate}$ is 30%).

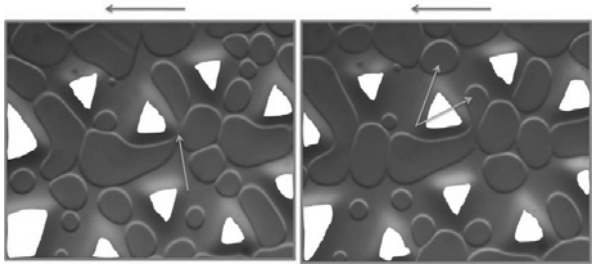

Figure 5. Upstream ganglion subdivision where LP is stretching at a junction and is then pinched off which leads to ganglion splitting for 1.5 mN/m IFT. The micromodel is MM1 and $F_{condensate}$=30%

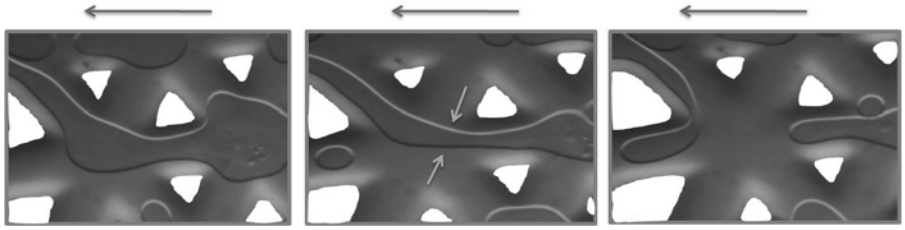

Figure 6. LP distortion (deformation) and snap-off mechanism for 1.5 mN/m IFT. The micromodel is MM1& $F_{condensate}$=30%.

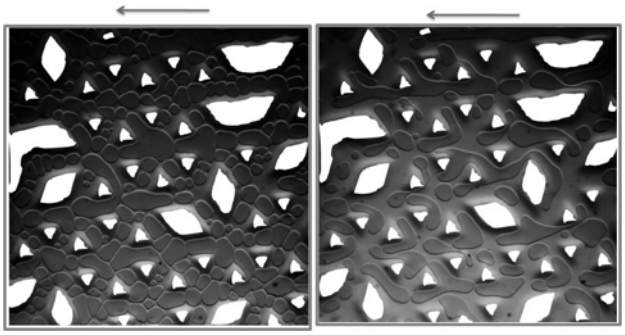

Figure 7. Flow is more emulsion-like for 1.5 mN/m IFT(left) and is more ganglion-like with less snap-off for 0.1 mN/m IFT (right). The micromodel is MM1 and $F_{condensate}$=30%.

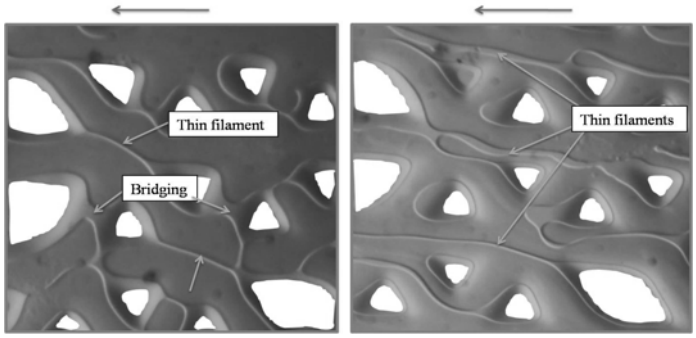

Figure 8. At low condensate saturation, pore hopping and filament flow of condensate are more efficient with more condensate bridging for higher IFT (1.5 mN/m) (left). The right picture is at 0.1 mN/m. The micromodel is MM1 & $F_{condensate}$=2%.

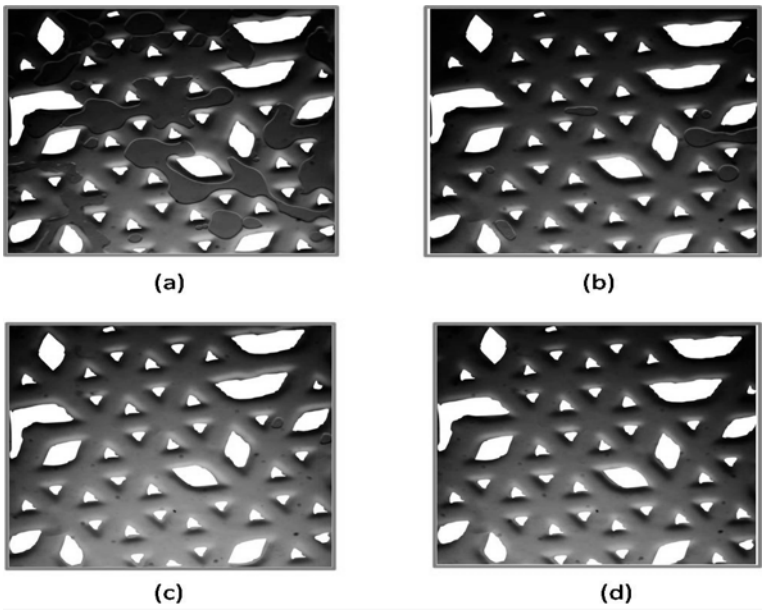

Figure 9. Light phase (gas) residual saturation. As IFT decreases, the gas residual saturation (blue) decreases. (a) 24.2 mN/m (b) 1.5 mN/m (c) 0.6 mN/m (d) 0.1 mN/m. MM1 micromodel is used.

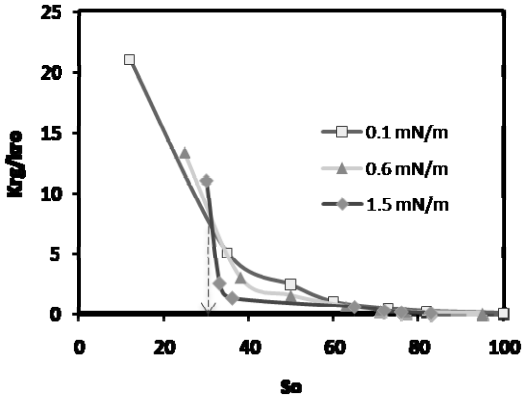

Figure 10. Plot shows the ratio (kr_g/kr_o) versus condensate saturation (S_o) for different interfacial tensions.

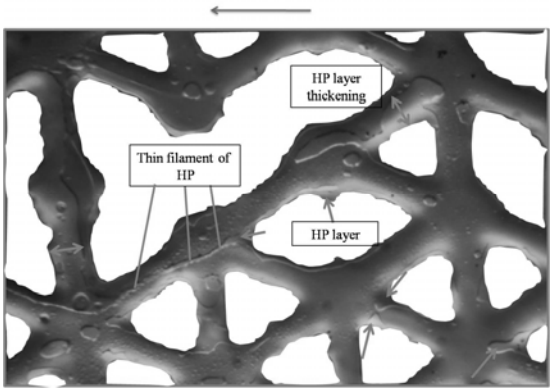

(a)

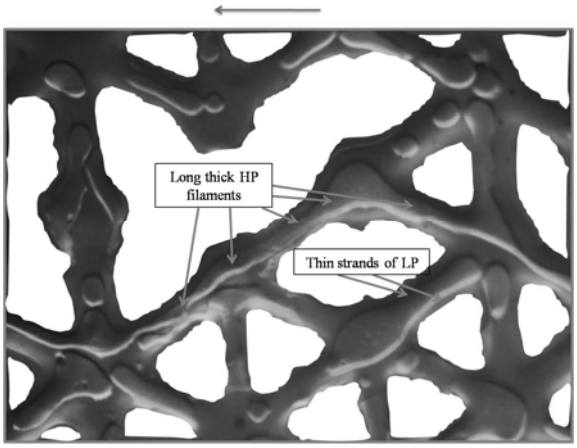

(b)

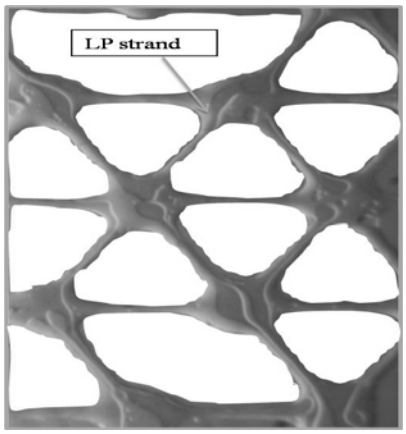

(c)

Figure 11. Pictures show filament flow and pore hopping of condensate are more efficient flow mechanisms for porous media of smaller pores. (a) and (b) MM2 (c) MM3

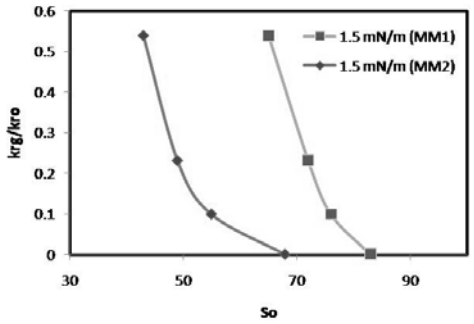

Figure 12. Ratio (kr_g/kr_o) versus condensate saturation (S_o) for two micromodels at 1.5 mN/m: a micromodel of large pores (MM1) and a micromodel of small pores (MM2)

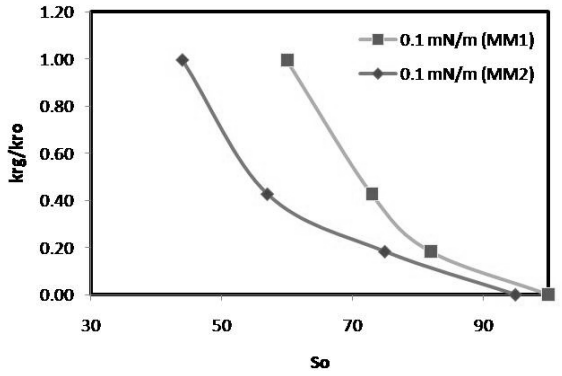

Figure 13. Ratio (kr_g/kr_o) versus condensate saturation (S_o) for two micromodels at 0.1 mN/m: a micromodel of large pores (MM1) and a micromodel of small pores (MM2).

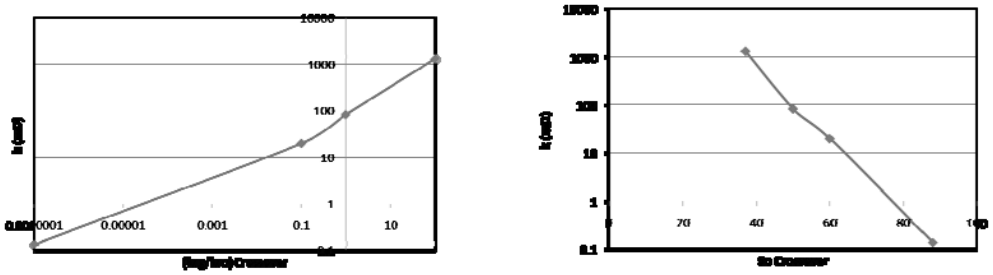

Figure 14. Plots show the relationship between permeability and crossover point where a change in gas condensate behavior occurs: (left) kr_g/kr_o crossover (right) condensate saturation (S_o) crossover.

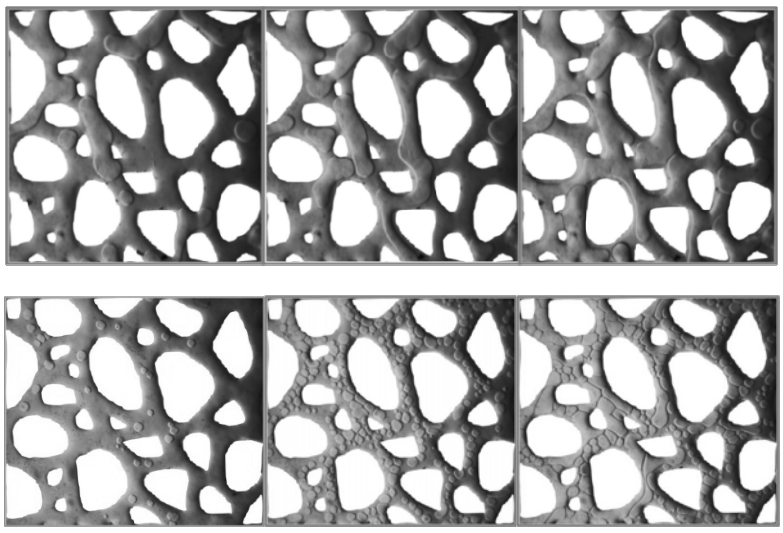

Figure 15. Pictures of light-wet micromodel. Upper row pictures show ganglion-like flow with hard deformation for 1.5 mN/m whereas the lower row pictures show more emulsion-like flow for 0.1 mN/m. The pictures are at $F_{condensate}$= 30%, 50% and 70% from left to right respectively.